

## Mid-infrared atmospheric transmittance at 5100 m-altitude Ali Observatory

Fei-Xiang Wang<sup>1,2</sup>, Fang-Yu Xu<sup>\*1</sup>, Jie Guo<sup>\*2</sup>, Zhi-Jun Zhao<sup>\*4,1</sup>, Rui-Ting Hao<sup>2</sup>, Jian-Guo Xiao<sup>3</sup>, Yu-Chao Jia<sup>3</sup> and Shan-Jie Huang<sup>1</sup>

<sup>1</sup> Yunnan Observatories, Chinese Academy of Sciences, Kunming 650216, China; [xu\\_fangyu@ynao.ac.cn](mailto:xu_fangyu@ynao.ac.cn), [zhaozhijun@htu.edu.cn](mailto:zhaozhijun@htu.edu.cn)

<sup>2</sup> Yunnan Key Laboratory of Optic-electronic Information Technology, Yunnan Normal University, Kunming 650092, China; [ynmugj@sohu.com](mailto:ynmugj@sohu.com)

<sup>3</sup> Yunnan KIRO-CH Photonics Co. Ltd, Kunming 650217, China

<sup>4</sup> School of Physics, Henan Normal University, Xinxiang 453007, China

Received 2020 January 9; accepted 2020 March 30

**Abstract** Ali in Tibet, 5100 m above sea level, is one of the most suitable locations in the world for infrared spectral observations. The atmospheric transmittances at Ali Observatory and Mauna Kea Observatory were calculated by MODTRAN using radiosonde data. The results were 0.848 and 0.789 respectively which indicated better conditions at Ali Observatory. A self-made instrument with a 320×256-pixel HgCdTe infrared focal plane array and a 7.5-cm diameter telescope was utilized for the actual measurements. Without the help of standard stars, the on-site and real-time atmospheric transmittance can be obtained as 0.831 by fitting the relation between the measured atmospheric radiation intensity and the zenith angle based on radiation transfer equations. This paper firstly reports the atmospheric transmittance in the  $M'$  band (4.605–4.755  $\mu\text{m}$ ) at the 5100 m-altitude Ali observatory by actual measurement. It shows that the high-altitude Ali observatory with sufficiently low water vapor content is suitable for observation in the mid-infrared bands.

**Key words:** infrared — atmospheric effects — radiation mechanisms: thermal

### 1 INTRODUCTION

The Ali Observatory is located at the mid-latitudes with an altitude of 5100 m where the atmosphere is dry and highly transparent, which make it a world-class observatory. Since 2003, Yao et al. have conducted a field survey at the Ali area and confirmed that the Ali Observatory is one of the best places for astronomical observations in East Asia (Yao et al. 2012). The Ali Observatory was selected as a candidate site for the Northern Cherenkov Telescope Array, the Thirty Meter Telescope and the Chinese Large Optical/infrared Telescope (Qian et al. 2018). However, there are few reports about the infrared atmospheric transmittance at Ali, although the percentage of photometric nights, atmospheric seeing and perceptible water vapor (PWV) have been studied for a few years.

Atmospheric transmittance in the infrared range is an important factor affecting infrared detection of spatial targets in military and astronomical observation applications, such as infrared warning, searching and infrared tele-

scope involved in ground operations. Generally, there are two main methods to obtain infrared atmospheric transmittance: the simulation method based on radiosonde data and actual measurement method. Many software packages like LOWTRAN, MODTRAN and LBLRTM have been employed for calculating the infrared atmospheric transmittance (Berk et al. 1999). At present, LBLRTM is an internationally recognized method with the highest calculation accuracy. In China, a set of combined atmospheric radiative transfer (CART) models was developed by Wei et al. (2007), which could estimate the infrared atmospheric transmittance with a relative error between 10% and 15%. However, real-time atmospheric transmittance cannot be obtained using software.

The actual measurement can provide on-site and real-time atmospheric transmittance data, which are extremely important for astronomical observation. Currently, the actual measurement methods for infrared atmospheric transmittance reported in literatures generally use standard stars as references. Kindel et al. (2001) applied the Langley method to obtain the solar spectral irradiance and trans-

---

\* Corresponding author

mittance from 350 to 2500 nm by calibrating the solar radiation intensity. Wu et al. (2017) utilized a heterodyne spectrometer to measure high-resolution transmittance in the infrared range of 4.479  $\mu\text{m}$ , regarding the Sun as the standard source. Bhattacharyya et al. (1990) and Liou & Bohren (1981) acquired the atmospheric transmittance by measuring the radiance of infrared standard stars at different zenith angles. However, these methods can only be measured during the day or night, but not both.

In this paper, MODTRAN software was used to simulate atmospheric transmittance in the infrared band at Ali and Mauna Kea. In addition, the atmospheric radiation at Ali was firstly actually measured on October 25 in 2017 and the atmospheric transmittance was calculated by fitting the curve between radiation and zenith angles based on the radiative transfer equation (RTE). The measurement method is independent of a standard star and is convenient to apply during both day and night.

## 2 SIMULATION BY MODTRAN SOFTWARE USING THE RADIOSONDE DATA

MODTRAN is an atmospheric radiation software package that is currently widely used in the calculation of atmospheric background radiation and atmospheric transmittance. In this paper, MODTRAN was utilized to calculate the atmospheric transmittance of Ali and Mauna Kea at 4.605–4.755  $\mu\text{m}$  to evaluate the  $M'$  band transmittance of the two places.

### 2.1 The Calculation Process

In the infrared band, several molecules such as  $\text{H}_2\text{O}$ ,  $\text{CO}_2$ ,  $\text{O}_3$  and  $\text{N}_2$  have a large impact on atmospheric transmittance. Since  $\text{H}_2\text{O}$  changes severely and irregularly with height, we relied on the radiosonde data from Lhasa (Ali does not have radiosonde data) at a 5 km altitude as the  $\text{H}_2\text{O}$  input in our calculations. The atmospheric profile of other molecules implement mid-latitude winter atmospheric models. Similarly, the radiosonde data from Hilo at a 4 km altitude near Mauna Kea were selected, and 1976 US standard models were applied for other molecules. The radiosonde data considered in this paper are from the “atmospheric soundings” website<sup>1</sup> established by the Department of Atmospheric Sciences at the University of Wyoming. Table 1 displays the atmospheric pressure, temperature and relative humidity varying with altitude at Lhasa and Mauna Kea on October 25 in 2017.

The input conditions at Ali are as follows: Type of Atmospheric Path: Slant Path to Space;  $\text{CO}_2$  Mixing Ratio: 380; Aerosol model: Rural-Vis= 23 km; Observer Height:

5 km; Zenith Angle  $0^\circ$ . The input conditions at Mauna Kea are the same except for the Observer Height (4.2 km). The result is plotted in Figure 1.

### 2.2 The Calculation Results and Analysis

Figure 1 displays the total atmospheric transmittance at wavelengths from 4.605  $\mu\text{m}$  to 4.755  $\mu\text{m}$  at Ali and Mauna Kea. The calculated mean transmittance, signified as the black dashed line in Figure 1 at Ali, is 0.848 on December 25 in 2017 while it is 0.789 at Mauna Kea on the same day, where the weather was sunny in both places. To investigate the difference, separate atmospheric transmittances of  $\text{H}_2\text{O}$ ,  $\text{CO}_2$ ,  $\text{O}_3$  and  $\text{N}_2$  molecules at the two places are shown in Figure 2.

In the  $M'$  band, the transmittances of  $\text{CO}_2$ ,  $\text{O}_3$  and  $\text{N}_2$  at Ali and Mauna Kea are close, but the transmittance of  $\text{H}_2\text{O}$  is obviously different. PWV is one of the key factors for ground-based astronomical observations in the infrared wavelength bands (Giovannelli et al. 2001; Otárola et al. 2010). The content of PWV in the atmosphere is related to temperature and relative humidity. According to Table 1, we calculated PWV at Ali and Mauna Kea on October 25 in 2017 as displayed in Table 2.

From Table 2, we can see that the PWV of Ali is lower than Mauna Kea at the same altitude. Above 5 km, the difference in water between the two places is 1.06 mm. However, the total PWV content at Mauna Kea is 3.46 mm more than at Ali. It can be inferred that the main factor affecting the transmittance is the PWV content of 4.2–5 km. However, we only calculated the PWV on October 25. Qian et al. compiled detailed reports on the precipitation at Ali Observatory, and Table 3 shows a comparison of median PWV values at the Ali Observatory with those at other excellent observatories around the world (Qian et al. 2018).

From Table 3, we can see that the annual PWV of Ali Observatory is less than that of most observatories, and comparable to the value at Mauna Kea. We re-simulated the atmospheric transmittance of Mauna Kea, where the Observer Height is 5 km, with MODTRAN, and the comparison with the results at Ali Observatory is depicted in Figure 3.

Figure 3 demonstrates that the average atmospheric transmittance at the 5 km altitude at Mauna Kea is calculated to be 0.852, which is very close to that at Ali. Similarly, the atmospheric transmittance relating to  $\text{H}_2\text{O}$  absorption is also very close. Therefore, the reason why Mauna Kea’s atmospheric transmittance is not as good as Ali’s may be that Ali’s altitude is higher than Mauna Kea. From the above research, we can find that although the PWV is one of the main factors affecting infrared atmospheric transmittance

<sup>1</sup> <http://weather.uwyo.edu/upperair/sounding.html>

**Table 1** The Radiosonde Data from Lhasa and Mauna Kea

Ali (Lhasa)				Mauna Kea			
HGHT (m)	PRES (atm)	TEMP (K)	RELH (%)	HGHT (m)	PRES (atm)	TEMP (K)	RELH (%)
5800	0.493	267.05	17	4267	0.603	276.65	85
7490	0.394	250.85	53	5880	0.493	268.45	19
9550	0.296	238.65	13	7432	0.403	258.85	18
10820	0.246	234.85	10	9686	0.297	242.45	88
12187	0.201	226.15	9	10926	0.248	232.45	58
12320	0.197	225.25	9	12228	0.204	221.85	58
14160	0.148	214.05	9	12450	0.197	219.85	48
116620	0.098	200.45		14240	0.148	204.65	36
17669	0.082	197.45		16600	0.098	198.45	33
18720	0.069	204.45		17678	0.082	199.35	31
20770	0.049	211.45		18789	0.068	199.25	28
23980	0.029	218.45		20700	0.049	211.05	9
26580	0.019	220.85		23880	0.029	217.25	1
				26480	0.019	220.45	1

**Table 2** The PWV at Different Heights at Ali and Mauna Kea

	4.2 km above	5 km above	9 km above	10 km above	12 km above	14 km above
Ali		2.28 mm	0.28 mm	0.14 mm	0.03 mm	0.008 mm
Mauna Kea	5.74 mm	3.22 mm	1.98 mm	0.37 mm	0.11 mm	0.02 mm

**Table 3** The PWV Values at Ali Observatory Compared to Those at Other Observatories

Station	Altitude (m)	PWV (mm)	Latitude	Longitude
Ali-A	5050	2.0	32.30 °N	80.05 °E
Ali-B	5250	1.8		
Ali-E	6000	1.2		
La Palma	2396	3.97	38.76 °N	17.89 °W
Greenland Summit	3216	1.28	72.57 °N	38.46 °W
Mauna Kea	4050	1.86	19.83 °N	155.48 °E
Hanle	4500	4.2	32.78 °N	78.96 °E
La Silla	2400	3.7	29.25 °S	70.73 °W
Paranal	2635	2.5	24.63 °S	70.40 °W
Chajnantor	5059	1.2	23.02 °S	67.75 °W

tance, when the PWV is similar, the altitude becomes an important factor. We thus suggest that the Ali Observatory could offer good atmospheric transmittance condition for infrared observations in the northern hemisphere.

### 3 ACTUAL MEASUREMENT BASED ON RADIATION TRANSFER EQUATION

On 2017 October 25, Ali's atmospheric radiation was measured by a self-made infrared telescope, and the atmospheric transmittance of the  $M'$  band at Ali Observatory was firstly obtained following the associated measurement method.

#### 3.1 Measuring Principle

For infrared radiation, the atmosphere is a medium with small absorption and scattering effect. As is known, the

monochromatic RTE could be expressed as follows

$$L_{\lambda}^{\text{out}} = L_{\lambda}^{\text{in}} e^{-\beta_0} + \int_0^{\beta_0} e^{-\beta} S_{\lambda}(\beta) d\beta, \quad (1)$$

where  $L_{\lambda}^{\text{out}}$  is the radiance of the ground reception,  $L_{\lambda}^{\text{in}} e^{-\beta_0}$  is the radiance of other radiation sources except the atmosphere (at a given wavelength),  $\beta_0$  is the optical thickness throughout the atmosphere and  $S_{\lambda}(\beta)$  is the source function at wavelength  $\lambda$ . When  $L_{\lambda}^{\text{in}} = 0$ , the atmosphere's spontaneous radiation is

$$L_{\lambda} = \int_0^{\beta_0} e^{-\beta} S_{\lambda}(\beta) d\beta. \quad (2)$$

Because  $S_{\lambda}(\beta)$  varies continuously with optical thickness, according to the mean value theorem for integrals, the following equation is established via  $S_{\lambda}(\beta')$

$$L_{\lambda} = S_{\lambda}(\beta') \int_0^{\beta_0} e^{-\beta} d\beta = S_{\lambda}(\beta') (1 - e^{-\beta_0}). \quad (3)$$

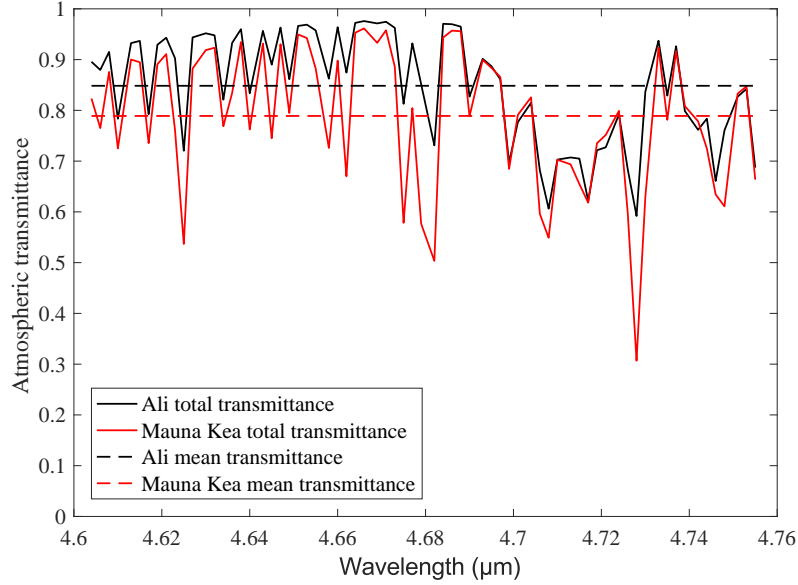


**Fig. 1** The atmospheric transmittance from MODTRAN.

Equation (3) establishes the relationship between spontaneous emission of the atmosphere and optical thickness at a certain wavelength. By Equation (1) when  $L_{\lambda}^{in} = 0$ , the zenith atmospheric transmittance  $\tau_{\lambda}$  can be expressed as

$$\tau_{\lambda} = \frac{L_{\lambda}^{out}}{L_{\lambda}^{in}} = e^{-\beta_0}. \quad (4)$$

In order to calculate the value of transmittance in a certain wavelength range, substituting  $\tau_{\lambda}$  into Equation (3), the relationship between atmospheric radiation and atmospheric transmittance in a certain wavelength range can be obtained by integrating the radiance in the desired wavelength

$$L_{\lambda} = \int_{\Delta\lambda} S_{\lambda}(\beta'')(1 - \tau_{\lambda}) d\lambda. \quad (5)$$

Within the width of the passband, according to the mean value theorem for integrals, Equation (6) is established via  $S_{\lambda}(\beta'')$

$$\begin{aligned} L_{\Delta\lambda} &= S(\beta'') \int_{\Delta\lambda} (1 - \tau_{\lambda}) d\lambda \\ &= S_{\lambda}(\beta'') \Delta\lambda \left(1 - \frac{1}{\Delta\lambda} \int_{\Delta\lambda} \tau_{\lambda} d\lambda\right). \end{aligned} \quad (6)$$

Let  $\bar{\tau}_0 = \frac{1}{\Delta\lambda} \int_{\Delta\lambda} \tau_{\lambda} d\lambda$  indicate the average transmittance of the wavelength, then Equation (6) becomes

$$L_{\Delta\lambda} = S(\beta'') \Delta\lambda (1 - \bar{\tau}_0). \quad (7)$$

It is assumed that the horizontal directions of the Earth's atmosphere at different heights are uniform, and the air quality follows the secant function of the zenith angle. When the atmospheric optics are thin, the relationship

between the average atmospheric transmittance  $\bar{\tau}$  and the zenith angle  $\theta$  is

$$\bar{\tau}_0 = (\bar{\tau})^{\sec \theta}. \quad (8)$$

Bringing Equation (8) into Equation (7) yields the relationship between radiation intensity, average atmospheric transmittance and zenith angle

$$L_{\Delta\lambda} = S(\beta'') \Delta\lambda [1 - (\bar{\tau})^{\sec \theta}]. \quad (9)$$

It must be mentioned that since this method does not consider the influence of scattering, it is only suitable for the case where atmospheric scattering is weak; in addition, this method is not suitable for cases with strong absorption peaks and high transmittance in the wavelength. Finally, this method needs to be measured in clear, cloudless weather. Since this method calculates the average value in the band, an approximate result is obtained.

### 3.2 Measuring Instrument

The equipment utilized in this work was a self-made infrared radiation measuring device. The optical system of the measuring device is a refracting telescope with a diameter of 7.5 cm, focal length of 15 cm and  $f$ -number of 2. The detector incorporates a  $320 \times 256$ -pixel deep-cooled HgCdTe infrared focal plane array. The spectral response of the detector is  $3.7\text{--}4.8 \mu\text{m}$ . After the device is added with a filter, it works in the astronomical  $M'$  band, which is  $4.605\text{--}4.755 \mu\text{m}$ . In order to control spontaneous emission of the device, a multi-stage refrigeration temperature control system is installed. The optical system and the detection system are respectively placed in two heat insulated

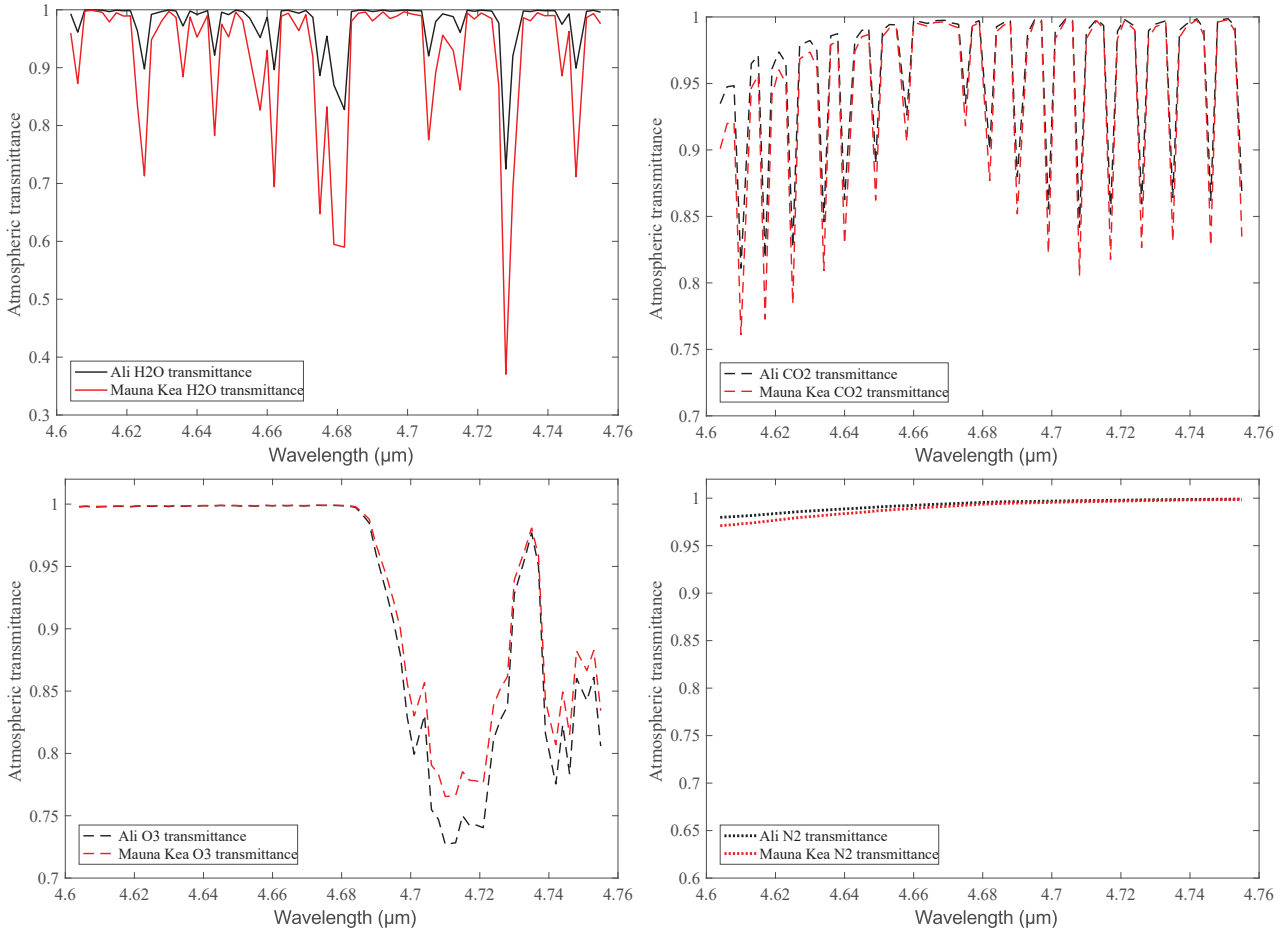


**Fig. 2** The atmospheric transmittances of H<sub>2</sub>O, CO<sub>2</sub>, O<sub>3</sub> and N<sub>2</sub>.

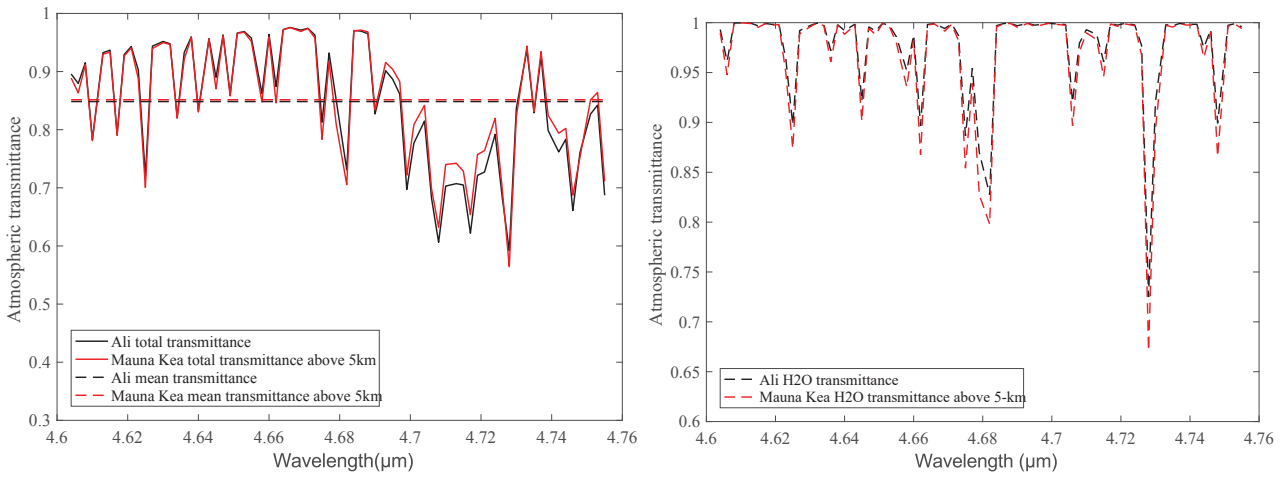


**Fig. 3** Atmospheric transmittance at Mauna Kea 5 km above sea level.

boxes, and three semiconductor cooling sheets are attached to the boxes. The hot place associated with the semiconductor refrigerating sheet is cooled by a compressor. After multi-stage cooling, the temperature inside the heat insu-

lated box can be lowered to  $-40^{\circ}\text{C}$ , and the temperature stability in the box is better than  $\pm 0.02^{\circ}\text{C}$ .

Infrared radiation in Ali Observatory was measured at intervals of several hours during the night under sunny and cloudless weather conditions on 2017 October 25.



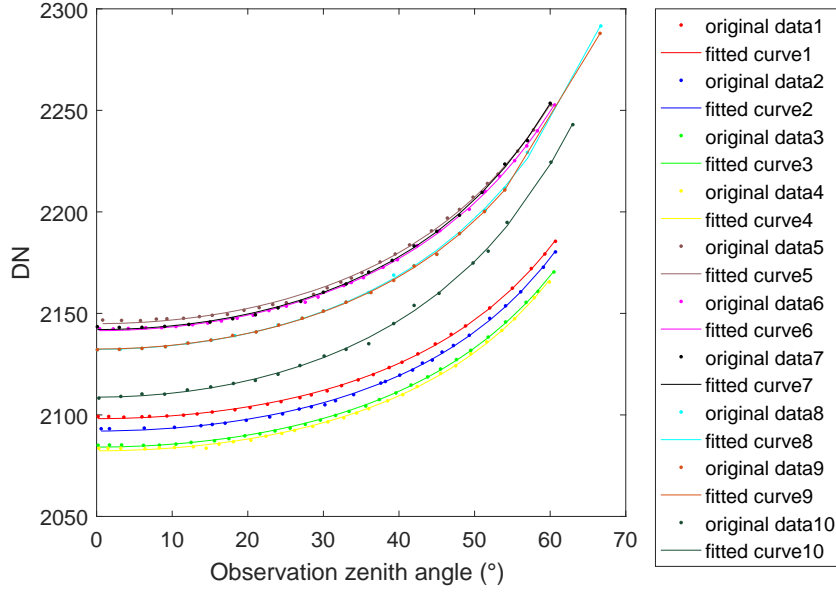


**Fig. 4** The relationship between instrument output and zenith angle.

The measurement was performed from  $0^\circ$  to  $60^\circ$  at intervals of  $3^\circ$ . Repeating the measurement ten times, the average radiation signal can be obtained. Chen et al. (2019) and Zhao et al. (2018) describe the instrument calibration process. The fitted relationship between the instrument output value  $DN$  and the radiation signal after blackbody calibration is

$$DN = 4.875 \times 10^5 L_{\text{signal}} t + 8.49 \times 10^3 L_{\text{amb}} t + 2.5492t + 707.00, \quad (10)$$

where  $DN$  is the output digital number from the  $320 \times 256$ -pixel infrared focal plane array focal plane detector in the instrument,  $t$  is the fixed integration time and  $L_{\text{signal}}$  is the blackbody radiance substituting the atmosphere radiance  $L_{\Delta\lambda}$ .  $L_{\text{amb}}$  is the ambient radiance. In Equation (10) on the right side, the first term represents the response to atmospheric radiation, the second term indicates the response to ambient radiation, especially instrument radiation, the third term is the other remaining response, such as the detector dark current, and the fourth term is the intercept term of the detector background response. To reduce ambient infrared radiation, the instrument was cooled down to  $-40^\circ\text{C}$ . When fixing  $L_{\text{amb}}$  and  $t$ , the last three terms can be taken as constant.

### 3.3 Data Processing and Discussion

According to Equation (9) and Equation (10), the relationship between instrument output  $DN$  and atmospheric transmittance  $\bar{\tau}$  as well as zenith angle  $\theta$  is

$$DN = a[1 - (\bar{\tau})^{\sec\theta}] + b, \quad (11)$$

where  $a$  and  $b$  are fitted constants. Then the atmospheric transmittance  $a, b, \bar{\tau}$  can be directly fitted by Equation (11).

To reduce random noise, we firstly average the pixels of each frame and then average the pixels of multiple-frames to obtain the output  $DN$ . The instrument output  $DN$  changes with zenith angle as depicted in Figure 4. The data were fitted applying Equation (11) with the least-squares method. Table 4 displays the results of each factor obtained by fitting.

The fitted average atmospheric transmittance was 0.831, with 95% confidence bounds, which is only 2% lower than the MODTRAN calculation result of 0.848. It can be seen that our actual measurement results are quite accurate. From Table 4, it can be ascertained that Ali's atmospheric transmittance constantly fluctuates with time. For example, within 6 minutes from 11:13 to 11:19, the fluctuation of transmittance is around 5.4%. What is more obvious is that the fluctuation of transmittance is around 7.5% in the short period from 17:03 to 17:05. The highest atmospheric transmittance at Ali was 8.8% higher than the lowest at the measurement time.

## 4 CONCLUSIONS

As one of the candidate sites for an East Asian infrared observatory, the Ali Observatory has the unique advantage of 5100-m altitude and the average annual PWV is very low. This is the first article to report actual measurements of the atmospheric transmittance for Ali Observatory at mid-infrared wavelengths. The results are advantageous for Ali Observatory, and the conclusions on atmospheric transmittance at Ali Observatory are as follows:

**Table 4** The Result of Each Factor Obtained by Fitting of Ten Groups

Factor	Group									
	1	2	3	4	5	6	7	8	9	10
Time	11:13	11:15	11:18	11:19	16:40	16:43	17:03	17:05	19:02	19:06
a	678	753	584	729	784	679	917.5	688.3	676.8	714
b	1999	1994	1982	1984	2015	2006	2012	1994	1997	1965
$\bar{\tau}$	0.854	0.870	0.825	0.866	0.8316	0.802	0.859	0.799	0.800	0.799
	$\pm 0.050$	$\pm 0.055$	$\pm 0.045$	$\pm 0.070$	$\pm 0.070$	$\pm 0.040$	$\pm 0.070$	$\pm 0.045$	$\pm 0.015$	$\pm 0.065$

(1) The atmospheric transmittances of Ali Observatory and Mauna Kea Observatory were calculated using MODTRAN. The result of the Ali Observatory calculation is 0.848 and the atmospheric transmittance of Mauna Kea is 0.789, which is lower than that at Ali Observatory. About the PWV, the difference between the two places is 1.06 mm when the altitude is above 5 km, but the total PWV content differs by 3.46 mm. The main factor affecting the transmittance is the PWV content of 4.2–5 km.

(2) We simulated the atmospheric transmittance of Mauna Kea 5 km above sea level, and the result was 0.852, which is equivalent to Ali's atmospheric transmittance. The research results indicate that it is not only necessary to have dry conditions during the site selection process, but the altitude is important. When the PWVs are similar, the atmospheric transmittance is higher in places with high altitude.

(3) We measured the atmospheric radiation of the Ali Observatory with the self-made infrared telescope and calculated the atmospheric transmittance based on RTE. The result is 0.831, which is only 2% lower than the MODTRAN result of 0.848. This demonstrates the accuracy of our measurement. Our method does not require a standard star and can obtain atmospheric transmittance day and night.

(4) Atmospheric transmittance constantly fluctuates with time, and on-site and real-time atmospheric transmittance can only be obtained by actual measurement.

The results from the conclusions could suggest that the high atmospheric transmittance of Ali Observatory in the mid-infrared wavebands will demonstrate the best conditions suitable for observations for future ground-based infrared telescopes. Therefore, the Ali Observatory might be a promising site in the northern hemisphere for astronomi-

cal observations.

**Acknowledgements** This work was funded by the National Natural Science Foundation of China (Grant Nos. 11673064, 11803089, U1931124).

## References

- Berk, A., Anderson, G. P., Bernstein, L. S., et al. 1999, in Society of Photo-Optical Instrumentation Engineers (SPIE) Conference Series, 3756, MODTRAN4 Radiative Transfer Modeling for Atmospheric Correction, Proc. SPIE, ed. A. M. Larar, 348
- Bhattacharyya, J. C., Scaria, K. K., Singh, J., Babu, G. S. D., & Nair, R. M. 1990, Bulletin of the Astronomical Society of India, 18, 1
- Chen, S., Xu, F., Wang, F., Yuan, X., & Luo, Y. 2019, Acta Optica Sinica, 39, 0301001 (in Chinese)
- Giovanelli, R., Darling, J., Henderson, C., et al. 2001, PASP, 113, 803
- Kindel, B. C., Qu, Z., & Goetz, A. F. H. 2001, Appl. Opt., 40, 3483
- Liou, K. N., & Bohren, C. 1981, Physics Today, 34, 66
- Otárola, A., Travouillon, T., Schöck, M., et al. 2010, PASP, 122, 470
- Qian, X., Yao, Y., Wang, H., et al. 2018, PASP, 130, 125002
- Wei, H. L., Chen, X. H., Zhan, J., & Rao, R. Z. 2007, Journal of Atmospheric & Environmental Optics, 2, 472
- WU, Q.-C., Huang, Y.-B. & Tan, T. 2017, Spectroscopy and Spectral Analysis, 06, 23 (in Chinese)
- Yao, Y.-Q., Wang, H.-S., Alvarez, M., et al. 1992, in Proc. of SPIE, 255, 139
- Zhao, Z.-J., Xu, F.-Y., Wei, C.-Q., et al. 2018, Infrared Technology, 307(07), 97 (in Chinese)